

Solvent induced phase transformations of ZIF-L to ZIF-8 and their derivatives^a

gas sensing properties

Xiaojie Wang ^a, Zifan You ^a, Hao Ding ^a, Yuchao Zhu ^a, Xiao Jia ^{a*}

^aCollege of Chemistry, Qishan Campus, Fuzhou University, Fuzhou, Fujian 350116, P. R. China

*Corresponding authors.

Tel.: +86-591-22867963

E-mail: jiaxiao@fzu.edu.cn (X. Jia)

Supporting Information

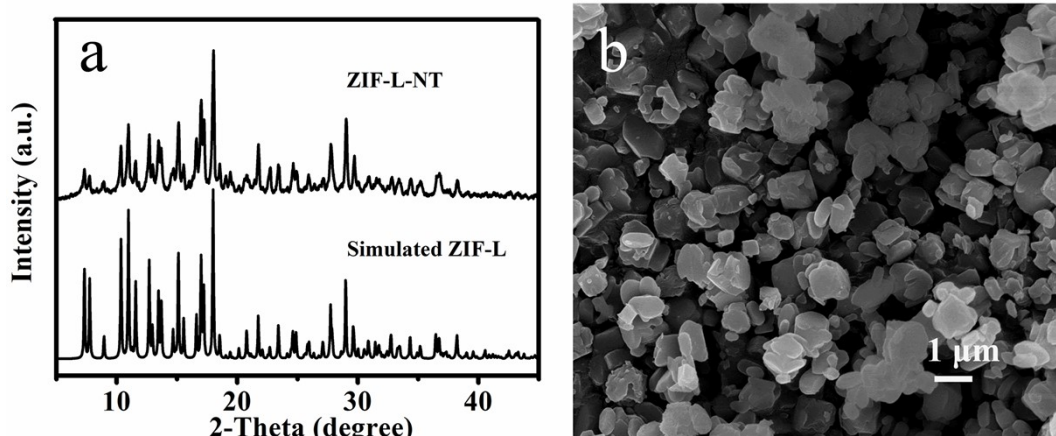


Fig. S1 XRD pattern (a), and FESEM image (b) of ZIF-L-NT.

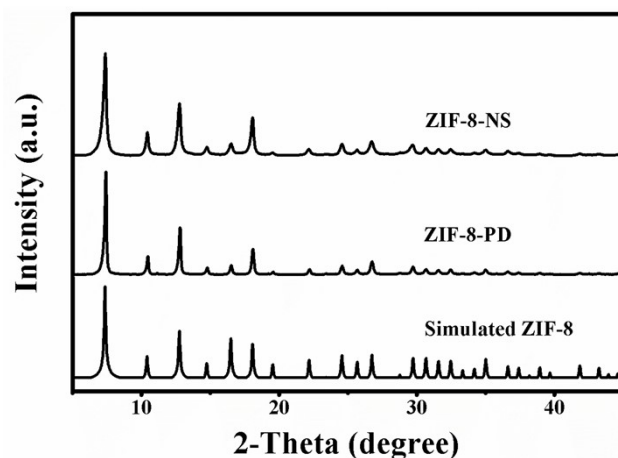


Fig. S2 XRD patterns of ZIF-8-NS and ZIF-8-PD.

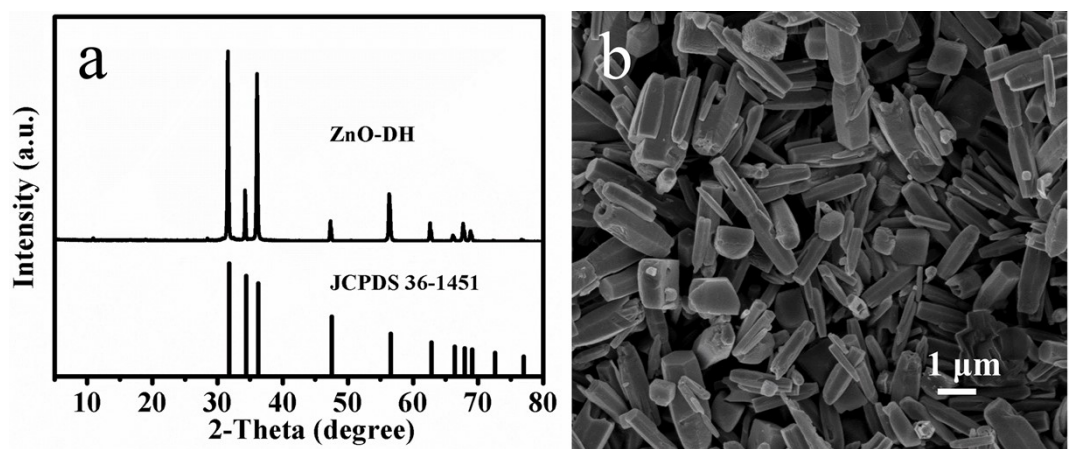


Fig. S3 XRD pattern (a), and FESEM image (b) of ZnO-DH.

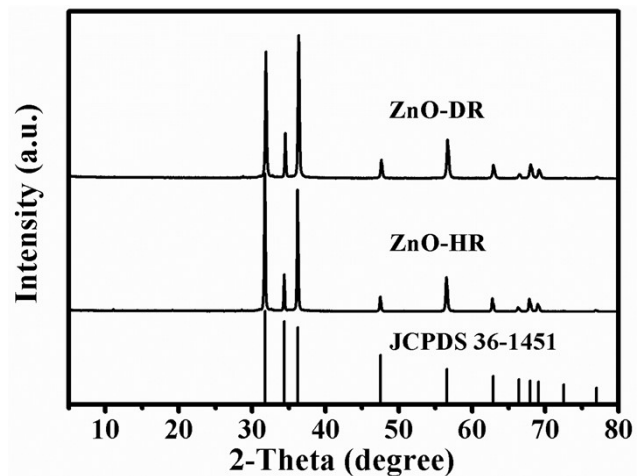


Fig. S4 XRD patterns of ZnO-DR and ZnO-HR.

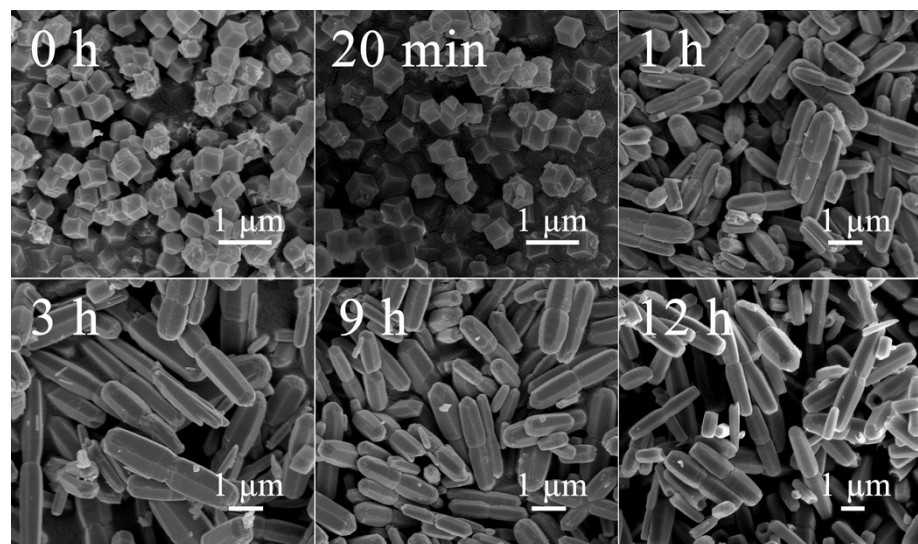


Fig. S5 FESEM images of ZnO-DR prepared with different time.

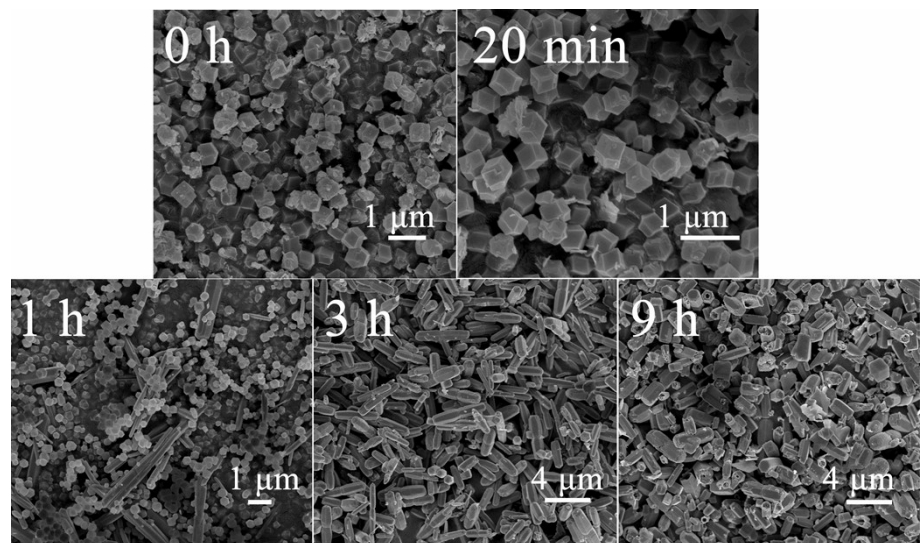


Fig. S6 FESEM images of the ZnO-HR prepared with different time.

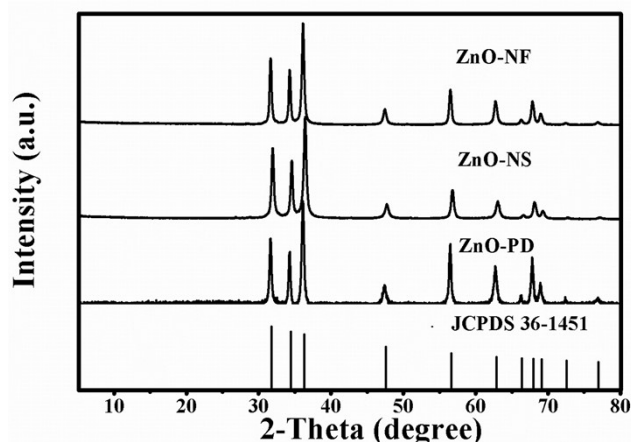


Fig. S7 XRD patterns of ZnO-NF, ZnO-NS and ZnO-PD.

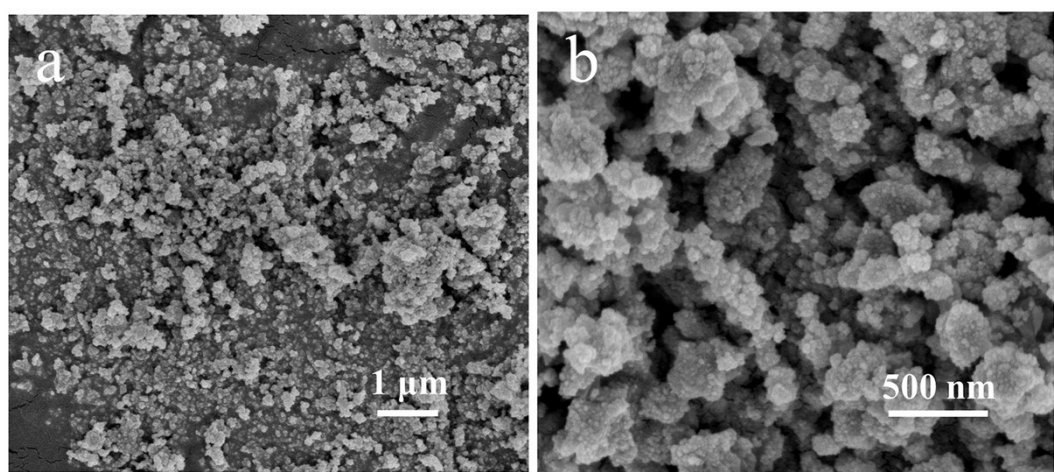


Fig. S8 Low (a) and high (b) magnification FESEM images of ZnO-NF.

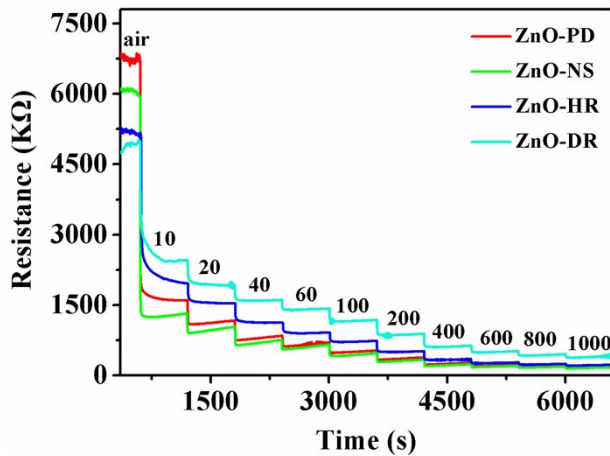


Fig. S9 Real-time response curves of as-fabricated gas sensors to various concentration of acetone vapor from 10 ppm to 1000 ppm at 300 °C.

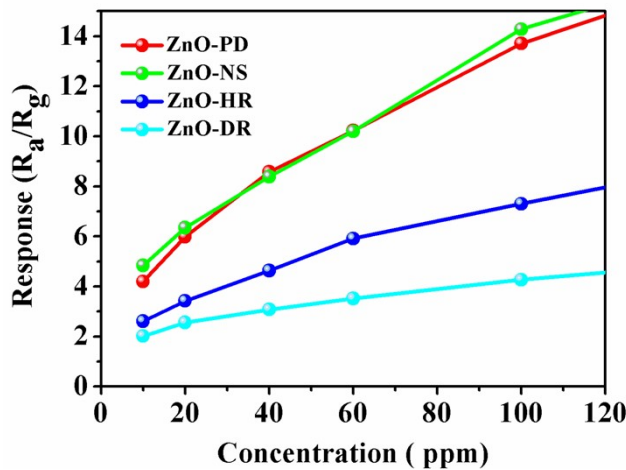


Fig. S10 Sensitivities of as-prepared samples to 10 ~100 ppm acetone vapor.

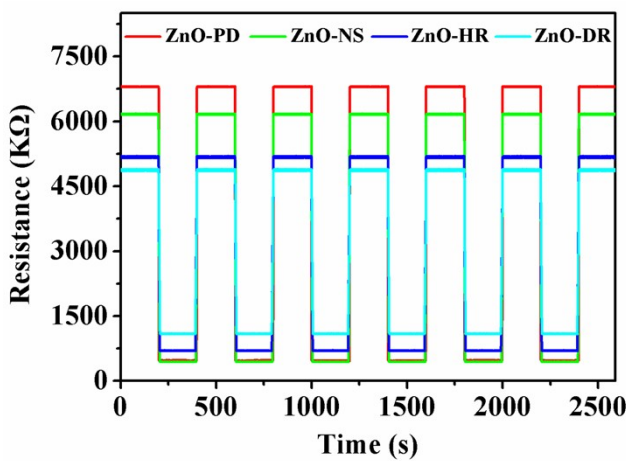


Fig. S11 Response-recovery curves of gas sensors to 100 ppm acetone vapor.

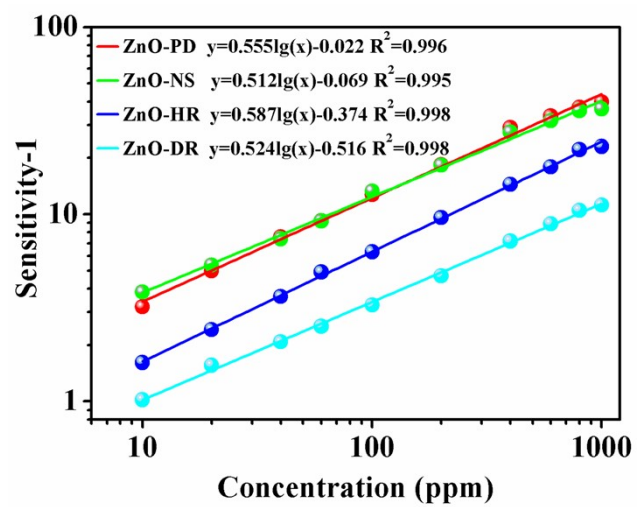


Fig. S12 Plots of $\log(S-1)$ versus $\log C$ for the as-prepared sensors to different concentrations of acetone vapor.